



Rescaled height coordinates for accurate representation of free-surface flows in ocean circulation models

Alistair Adcroft ^{*,1}, Jean-Michel Campin ²

Program in Atmospheres and Oceans and Climate, Massachusetts Institute of Technology, Cambridge, MA 02139, USA

Received 6 August 2003; received in revised form 12 September 2003; accepted 15 September 2003

Available online 7 November 2003

Abstract

Conventional height coordinate models have previously represented free-surface variations by a variable thickness upper layer. We present a rescaled height coordinate, which we call z^* , that treats the time-dependent free surface as a coordinate surface. This coordinate is isomorphic with the atmospheric η coordinate, sometimes known as the step-mountain coordinate. The z^* coordinate has also been used in a coastal ocean model. However, unlike both these implementations, here we use the finite volume method within the z^* coordinate framework, allowing an accurate representation of topography. The resulting scheme provides a very accurate representation of motions over steep topography in a three-dimensional general circulation model, even with fast and large amplitude free-surface variations.

© 2003 Elsevier Ltd. All rights reserved.

Keywords: Ocean model; Vertical coordinate; Coordinate transformation; Free surface; Internal wave generation; Topography

1. Introduction

Until recently there has been essentially three classes of ocean model based on their choice of vertical coordinate: (i) height coordinate models such as MOM4 (Griffies et al., 2003), the MIT ocean model (Marshall et al., 1997a) and POP (Smith et al., 1992); (ii) terrain following coordinate models such as ROMS (Haidvogel et al., 2000), SCRUM (Song and Haidvogel, 1994) and POM; and (iii) isentropic or isopycnal models such as MICOM (Bleck et al., 1992) and HIM

* Corresponding author.

E-mail addresses: adcroft@mit.edu (A. Adcroft), jmc@ocean.mit.edu (J.-M. Campin).

¹ Supported by the Office of Naval Research, grant N00014-03-1-0412.

² Supported by the M.I.T. Climate Modeling Initiative.

(Hallberg, 1997). With the recognition that each of these coordinate systems has its advantages and disadvantages, and that no single coordinate system is absolutely perfect for all applications, efforts are now underway to create generalized and hybrid coordinate models that can employ the appropriate coordinate in different regions of the ocean (Bleck, 2002; Song, submitted for publication). However, little attention is being paid to alternative coordinate systems despite the fact that a large set of vertical coordinates could be employed in general coordinate models. As yet only a small set of vertical coordinates have been explored. Here, we focus on a specific vertical coordinate which is essentially height based but shares some similarity with σ coordinates. However, it does not need the paraphernalia of a generalized vertical coordinate and can be implemented very easily in existing height coordinate models.

The coordinate, which we call “ z^* ”, was first introduced in a coastal application (Stacey et al., 1995). It is analogous to the meteorological η coordinate (sometimes known as the step-mountain coordinate) of Mesinger et al. (1988). The η coordinate was presented as an alternative for atmospheric σ -coordinate models that suffer from large pressure gradient errors (Janjic, 1977). However, it is not a terrain following coordinate and is in fact more closely related to a simple pressure coordinate. Like σ coordinates, the η coordinate does stretch with surface pressure variations. The lower boundary (ground) of an η coordinate model is not a constant coordinate surface (unlike in σ coordinates) but it *is* fixed in time so that the computational domain is unchanging with time. Similarly, the z^* coordinate transforms the moving boundary problem of the oceans free surface into a fixed domain.

The z^* coordinate does not address the representation of topography and so in Stacey et al. (1995) and Stacey and Gratton (2001) the topography was represented in the step mountain fashion of earlier height coordinate models. Use of the finite volume method for discretizing the model allows an accurate representation of topography by means of shaped volumes (“shaved cells”) or variable bottom layer thickness (partial cells) and have been demonstrated to overcome the inadequacies of height coordinates in representing topography (Adcroft et al., 1997; Pacanowski and Gnanadesikan, 1998).

The essential advantage of the particular coordinate transformation employed here is that it maps a time-dependent domain into a fixed domain. The time-dependent domain is due to the “free” surface which has been difficult to incorporate in ocean models (Killworth et al., 1991; Dukowicz and Dvinsky, 1993). Thus, to motivate the problem, we briefly describe the moving domain problem that confronts height coordinate models.

In a Boussinesq model, the continuity equation takes the form

$$\nabla_z \cdot \vec{v}_h + \partial_z w = 0$$

where $\vec{v}_h = (u, v, 0)$ is the horizontal flow vector, w is the vertical velocity and z is height. Sea surface height evolves according to the depth integrated continuity equation,

$$\partial_t \eta + \nabla \cdot (H + \eta) \langle \vec{v}_h \rangle = P - E$$

where $\langle \vec{v}_h \rangle = \frac{1}{H+\eta} \int_{-H}^{\eta} \vec{v}_h dz$ is the depth averaged flow and where we have used the boundary conditions

$$w_{z=\eta} = D_t \eta - (P - E) \quad \text{at } z = \eta(x, y, t) \quad (1)$$

$$w_{z=-H} = -\vec{v}_h \cdot \nabla H \quad \text{at } z = -H(x, y) \quad (2)$$

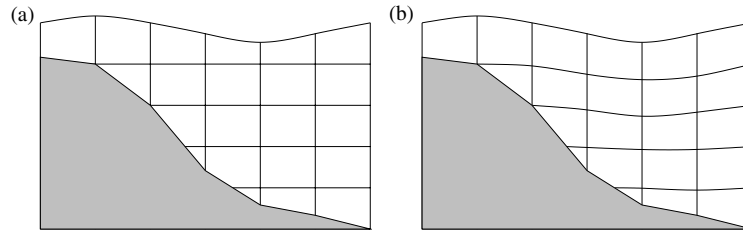


Fig. 1. (a) Schematic of use of a finite volume height coordinate model to represent a non-linear free surface. To avoid numerical instability (when the upper layer is too thin) one has to choose a nominal top level thickness larger than free-surface variations. (b) The z^* coordinate stretches the grid to follow the barotropic mode.

at the surface, $z = \eta$, and the bottom, $z = -H$. Here, $P - E$ is the excess precipitation over evaporation. Height coordinates, z , as used in models, are referenced to a time mean geoid and the free-surface displacement, η , moves relative to this coordinate system. If the free-surface dynamics are unapproximated³ then a height coordinate model must represent the free surface as a moving boundary. In Griffies et al. (2001) and Campin et al. (in press), this is implemented accurately by allowing the top model layer to vary in thickness, as shown schematically in Fig. 1. However, the approach has a serious limitation; free-surface variations must be smaller than the top layer thickness, Δz_1 , to ensure that the surface layer does not vanish,

$$\eta > -\Delta z_1$$

The model could be coded to allow the top layer to vanish (as happens in layer models) and the second layer then take on the role of surface layer with variable thickness but when this happens both the accuracy and stability are suspect. It is most likely difficult to make the transition of a vanishing layer smooth enough to not generate numerical problems; conservation issues would be a major concern and the likelihood of vanishing layers becomes more frequent with increasing vertical resolution. Thus we are motivated to examine alternatives to the variable thickness surface layer approach and in particular consider coordinate transformations as a way of treating the moving domain problem.

In Section 2, we describe the z^* coordinate, transformed equations and implementation in the MIT general circulation model (Marshall et al., 1997a). In Section 3, we illustrate the advantages of the z^* coordinate over height coordinates for a coastal scale application, modeling internal wave generation by barotropic tides interacting with topography. Finally, we discuss the wider potential and possibilities for z^* and related coordinates.

2. The rescaled height coordinate, z^*

Following Stacey et al. (1995), the coastal coordinate is defined as

³ The rigid-lid approximation and linearized free-surface method both approximate the position of the ocean surface as being at $z = 0$.

$$z^* = \sigma(x, y, z, t)H(x, y) = \frac{z - \eta(x, y, t)}{H(x, y) + \eta(x, y, t)}H(x, y) \quad (3)$$

where $z = H$ is the location of the solid bottom, x, y are horizontal coordinate, t is time and η is the free-surface displacement. σ is the conventional time-dependent terrain following coordinate. Despite the appearance of σ in the definition, the coordinate z^* is more closely related to height than a terrain following coordinate, as is apparent in Fig. 1.

We call the vertical velocity in this coordinate system “ w^* ” which is related to the fixed frame vertical velocity, “ w ”, by the relation

$$w^* \equiv D_t z^* = \frac{H}{H + \eta} \left(w - \left(1 + \frac{z^*}{H} \right) D_t \eta + \frac{z^* \eta}{H^2} \vec{v}_h \cdot \nabla H \right) \quad (4)$$

The location of the lower boundary is

$$z = -H(x, y) \Rightarrow z^* = -H(x, y) \quad (5)$$

and although this is not a constant coordinate surface, such as would be the case for a terrain following coordinate, it is fixed in time. The no normal flow boundary condition at the solid lower boundary becomes

$$w_{z=-H} = -\vec{v}_h \cdot \nabla H \Rightarrow w_{z^*=-H}^* = -\vec{v}_h \cdot \nabla H \quad (6)$$

where $\vec{v}_h = (u, v, 0)$ is the horizontal flow vector at $z = -H(x, y)$. The upper boundary is located at

$$z = \eta(x, y, t) \Rightarrow z^* = 0 \quad (7)$$

which, although the physical free surface is moving, is clearly fixed in time in the z^* frame. The overall computational domain is thus fixed in time and so the complicating issues concerning moving boundaries and vanishing layers do not arise.

The kinematic boundary conditions at the free surface become

$$w_{z=\eta} = D_t \eta - (P - E) \Rightarrow w_{z^*=0}^* = -\frac{H}{H + \eta} (P - E) \quad (8)$$

The hydrostatic, Boussinesq equations transformed into z^* coordinates are

$$\partial_t \vec{v}_h + \vec{v}_h \cdot \nabla_{z^*} \vec{v}_h + w^* \partial_{z^*} \vec{v}_h + f \hat{k} \times \vec{v}_h + \frac{1}{\rho_0} \nabla_{z^*} p + \frac{\rho}{\rho_0} \nabla_{z^*} \Phi = \vec{F} \quad (9)$$

$$\frac{1}{\rho_0} \partial_{z^*} p + \left(\frac{H + \eta}{H} \right) \frac{g\rho}{\rho_0} = 0 \quad (10)$$

$$\partial_t \left(\frac{H + \eta}{H} \right) + \nabla_{z^*} \cdot \left(\frac{H + \eta}{H} \vec{v}_h \right) + \partial_{z^*} \left(\frac{H + \eta}{H} w^* \right) = 0 \quad (11)$$

$$\partial_t \eta + \nabla \cdot \int_H^0 \left(\frac{H + \eta}{H} \vec{v}_h \right) dz^* = P - E \quad (12)$$

$$\partial_t \left(\frac{H + \eta}{H} \theta \right) + \nabla_{z^*} \cdot \left(\frac{H + \eta}{H} \theta \vec{v}_h \right) + \partial_{z^*} \left(\frac{H + \eta}{H} \theta w^* \right) = \frac{H + \eta}{H} Q \quad (13)$$

where \vec{v}_h is the horizontal component of flow, ρ_0 is a constant reference density, ρ is the in situ density, $\Phi = gz$ is the geopotential, p is pressure, g is the constant gravitational acceleration and θ is any arbitrary scalar such as potential temperature, salinity or a passive tracer. \vec{F} and Q are arbitrary forces and sources of tracers.

Both pressure and geopotential gradients appear in the horizontal momentum equations; this is a consequence of using a coordinate other than height or pressure. The appearance of two gradient terms raises the possibility of pressure gradient errors (Haney, 1991). However, unlike in terrain following coordinates, the geopotential gradient is small since the slope of the z^* coordinate surface is typically very small. Indeed, for the special case of a flat free surface there are no geopotential gradients and so no pressure gradient errors in the resting state. Thus, there will be no spontaneous generation of motion over topography from a resting state such as is common in terrain following coordinate models. Although potential pressure gradient errors are already small, compared to a terrain following coordinate model, those that remain can be reduced further by judiciously subtracting a reference state with constant density. The density is partitioned into a constant part and perturbation,

$$\rho = \rho_0 + \rho'(x, y, z^*, t)$$

and associated reference pressure, $p_0(z^*)$, defined to be in hydrostatic balance and equal to zero at the sea-surface, $z^* = 0$ (not at $z = 0$):

$$\partial_{z^*} p_0 = -g \left(\frac{H + \eta}{H} \right) \rho_0 \quad \text{and} \quad p_0(z^* = 0) = 0 \tag{14}$$

and perturbation pressure, $p' = p - p_0$, which must satisfy the boundary conditions:

$$\partial_{z^*} p' = -g \frac{H + \eta}{H} \rho' \quad \text{and} \quad p'(z^* = 0) = p_a$$

where p_a is the atmosphere loading (pressure at the sea surface). Solving (14) for p_0 we find

$$p_0(z^*) = p_0(x, y, z, t) = -g\rho_0 \frac{H + \eta}{H} z^* = g\rho_0(\eta - z) = g\rho_0\eta - \rho_0\Phi$$

The pressure and geopotential gradient terms can now be expanded

$$\begin{aligned} \frac{1}{\rho_0} \nabla_{z^*} (p_0 + p') + \frac{\rho'}{\rho_0} \nabla_{z^*} \Phi &= g\nabla\eta - \nabla_{z^*} \Phi + \frac{1}{\rho_0} \nabla_{z^*} p' + \frac{\rho_0 + \rho'}{\rho_0} \nabla_{z^*} \Phi \\ &= g\nabla\eta + \frac{1}{\rho_0} \nabla_{z^*} p' + \frac{\rho'}{\rho_0} \nabla_{z^*} \Phi \end{aligned}$$

so that the static and unchanging parts of the pressure gradient balance are hidden. The amplitude of the geopotential gradient term, $\nabla_{z^*} \Phi$, is now seen to be smaller by of order (ρ'/ρ_0) . The geopotential, $\Phi = gz$, can be eliminated since we know the function $z(z^*)$:

$$\nabla_{z^*} \Phi = g\nabla_{z^*} z = g\nabla_{z^*} \left(\eta + \frac{H + \eta}{H} z^* \right) = g\nabla_{z^*} \left(\eta \left(1 + \frac{z^*}{H} \right) \right)$$

Thus the horizontal momentum equation (9) can be rewritten as

$$\partial_t \vec{v}_h + \vec{v}_h \cdot \nabla_{z^*} \vec{v}_h + w^* \partial_{z^*} \vec{v}_h + f \hat{k} \wedge \vec{v}_h + g \nabla \eta + \frac{1}{\rho_0} \nabla_{z^*} p' + \frac{g \rho'}{\rho_0} \nabla_{z^*} \left(\eta \left(1 + \frac{z^*}{H} \right) \right) = \vec{F} \quad (15)$$

or as

$$\partial_t \vec{v}_h + \vec{v}_h \cdot \nabla_{z^*} \vec{v}_h + w^* \partial_{z^*} \vec{v}_h + f \hat{k} \wedge \vec{v}_h + \frac{g \rho}{\rho_0} \nabla \eta + \frac{1}{\rho_0} \nabla_{z^*} p' + \frac{g \rho'}{\rho_0} \nabla_{z^*} \frac{\eta z^*}{H} = \vec{F} \quad (16)$$

The difference between (15) and (16) is that the pressure gradient term is linear in (15), and is non-linear in (16). In our case, because we use an implicit-in-time treatment of the free surface, we choose the linear form (15).

2.1. Implementation in the MIT general circulation model

The new coordinate is implemented in the MIT General Circulation Model (MITgcm) by means of a general vertical coordinate. In formulating MITgcm, we deliberately made the vertical coordinate arbitrary to allow easy adoption of new coordinates but designed it to exactly recover the height coordinate algorithm described in Marshall et al. (1997a) and Adcroft et al. (1997). The continuous equations are derived in Appendix A. The time-dependent nature of the z^* coordinate means that the model layer thicknesses evolve in time. This evolution is analogous to the evolution of the surface layer thickness in the pure height coordinate model with non-linear free surface. Our algorithm then is just an extension of the free-surface method described in Campin et al. (in press) but applied to all model levels; the time-stepping of layer thicknesses, continuity and tracer equations are arranged so as to give accurate local and global conservation.

3. Illustration: internal wave generation by tidal flow on a continental slope

An illustrative example of how z^* is more natural coordinate for modeling flows with a significant barotropic component is the case of internal wave generation by interaction of the barotropic tide with topography.

We define a two-dimensional domain in the x - z plane with an open boundary to the west (off-shore) and closed to the east. The domain is 18 km wide and nominally $H = 200$ m deep. There are 300 points in the horizontal with resolution varying smoothly from 70 m down to a minimum of 35 m over the slope. In the vertical, the resolution is uniform at 10 m. At the closed boundary there is a 40 m deep coastal shelf which is 2 km wide separated from the deeper ocean by a linear continental slope with a 7% grade (see masked region in Fig. 2). The initial stratification is uniform such that $NH = 20 \text{ cm s}^{-1}$. The model is forced with a prescribed barotropic flow at the open boundary (initially zero and tending positive) that oscillates with amplitude 10 cm s^{-1} at the M2 tidal frequency. We use a linear equation of state with no salinity dependence. A third order direct space time method with a Sweby flux limiter (Hundsdoerfer et al., 1995; Pietrzak, 1998) is used for buoyancy advection. Consequently explicit diffusion can be set to zero. Explicit viscosity is isotropic and negligible (10^{-5} m s^{-2}) and does not affect the solution; we integrate the model until the internal waves reach the open boundary, after about 2 days. We use a time step of 120 s for all

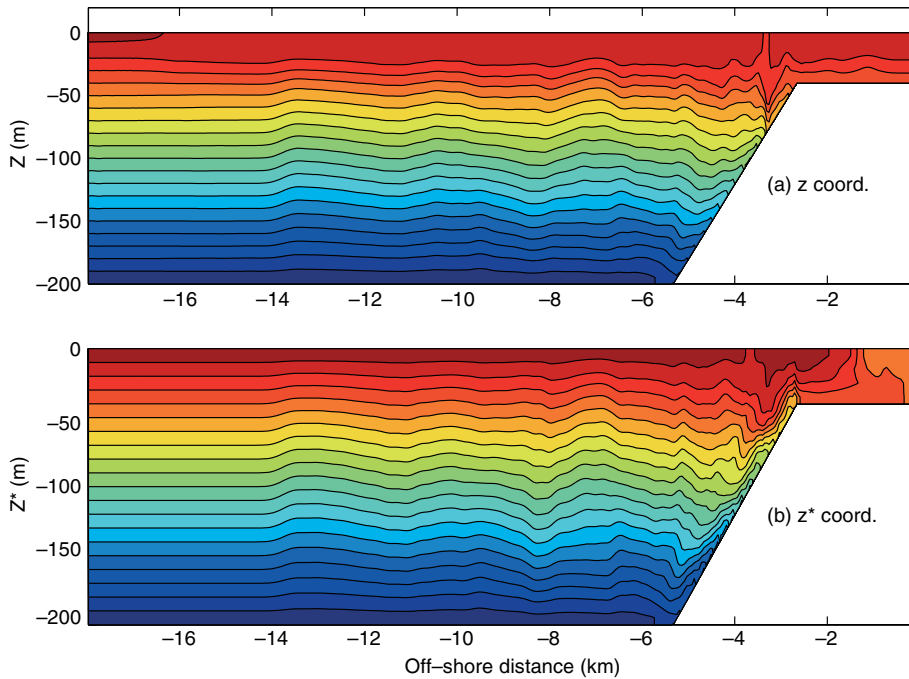


Fig. 2. Buoyancy field after five tidal periods for (a) the z coordinate model and (b) the z^* coordinate model. The vertical axis is the respective coordinate. Contour interval is $1 \times 10^{-5} \text{ m s}^{-2}$. Note the stronger upwelling signal over the slope in (b) and the relatively homogenized fluid in the top layer of (a).

modes (i.e. synchronous stepping with no splitting). In the height coordinate model, the free surface is treated as non-linear free surface as described in Campin et al. (in press).

In both the z and z^* coordinate models the response to the open boundary forcing is to adjust the barotropic model almost instantaneously; the interior flow matches the boundary flow and diverges so that the free surface is pushed up and down. The very fast adjustment time means there are negligible spatial gradients in the free surface so that the free surface heaves up and down coherently across the domain. Thus, in the upper layers of the z coordinate model, there is a vertical velocity associated with the free-surface motion which tapers to zero near the bottom. In the z^* coordinate model, motion associated with the pure barotropic mode is identically horizontal (along coordinate surfaces) with $w^* = 0$.

The constriction presented to the horizontal flow by the continental slope leads to a relative acceleration of flow over the slope and shelf. During the on-shore phase of the tidal forcing this leads to strong advection of deep water up the continental slope leading to a lateral buoyancy anomaly. As the tidal flow relaxes, the buoyancy anomaly adjusts under gravity and thus an internal wave is generated over the continental slope, which then propagates toward the open boundary. Fig. 2a and b shows the buoyancy after five tidal periods of integration for the z and z^* coordinate models respectively. Although the solutions are largely similar there are two key differences: (i) the strength of upwelling anomalies on the slope is stronger in the z^* model, leading to stronger internal waves emanating from the slope and (ii) there is erosion of stratification in the

surface layers of the z model which is due to a combination of strong vertical flows and a boundary effect associated with the non-linear free surface. Some differences are also apparent in structures on the coastal shelf but here the active processes include propagating bores, triggered by the upwelling anomalies, which are not properly resolved in this calculation.

Fig. 3 shows the evolution of buoyancy at a nominal depth of 95 m. In the height coordinate model, the buoyancy signal includes an oscillation associated with the heave of the basic stratification past the measurement point. This takes the form of the horizontal structures in panel (a) and significantly masks the internal wave signature. By interpolating the height coordinate model solution to a z^* surface ($z^* = -95$ m) we can effectively remove the barotropic heave signal, as shown in panel (b). The effect of the horizontal barotropic flow on the propagating internal waves is now obvious: while the tide is flowing on-shore the internal waves are arrested and then on the ebb tide are carried faster off-shore. The Froude number is $U/NH = 0.5$. The average phase speed of the waves, measured from the figures, is $11,000 \text{ m}/2 \text{ days} \sim 7 \text{ cm s}^{-1}$ which is approximately the same as NH/π . Panel (c) shows the z^* model solution. Here, it is even more evident that the z and

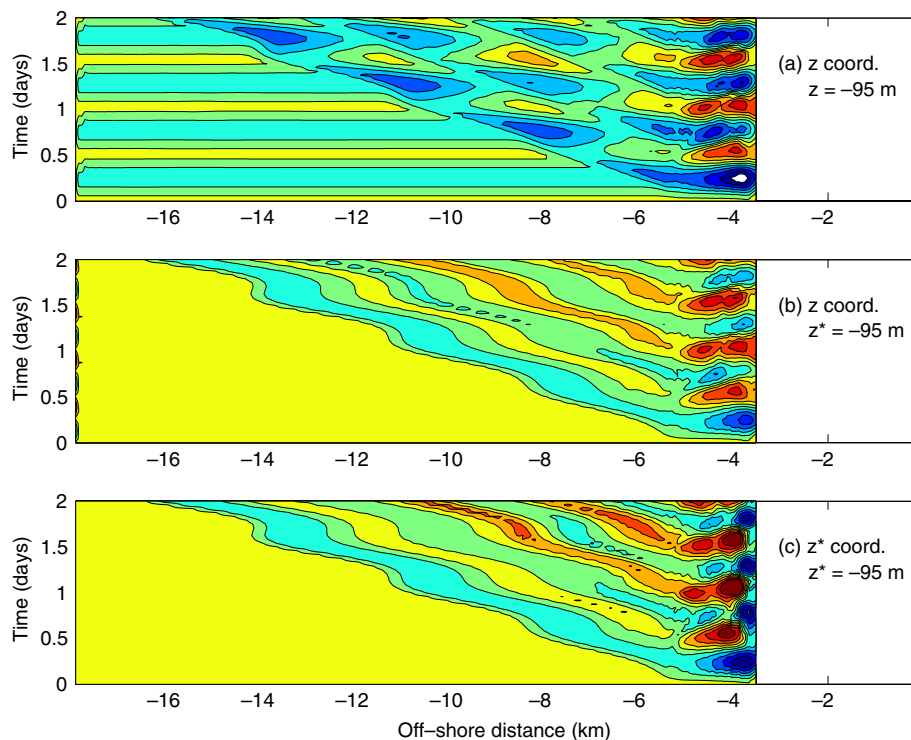


Fig. 3. Hovmueller diagrams for buoyancy at z or $z^* = -95$ m. Contour interval is $4 \times 10^{-6} \text{ m s}^{-2}$. Panel (a) is the z coordinate solution at $z = -95$ m and contains a strong signal associated with the heave of stratification past a point in space. (b) is as for (a) but interpolated to $z^* = -95$ m which neatly removes the barotropic heave signal. Advection of the internal wave signal by the barotropic flow is now apparent in the coordinate frame. (c) is the z^* solution at $z^* = -95$ m which should be compared with (b). Note the stronger internal wave signal both in the interior and near the slope region.

z^* models differ (panels b and c), with a stronger signal both at the source region (over the slope) and in the interior.

When such differences arise the question is raised as to which model is to be preferred. We chose not to embark on a prohibitive convergence study since this particular problem inherently becomes non-hydrostatic as the resolution is increased and we have not yet implemented the non-hydrostatic form of the model (Marshall et al., 1997b) in z^* coordinates. We will, however, offer some simple arguments in favor of the z^* coordinate model: in z coordinates the barotropic mode has, by necessity, a vertical flow associated with it. Any cross coordinate flow must ultimately lead to some diabatic contributions to the evolution simply due to the existence of truncation error. It is also evident that despite careful treatment of the non-linear free surface in z coordinates (Campin et al., in press) it is difficult to avoid a spurious boundary effect; the erosion of the surface layers occurs uniformly across the domain, independent of the internal waves. The same algorithm that was used to treat the variable surface layer in Campin et al. (in press) is used here to implement variable layer thicknesses in z^* coordinates. However, using z^* coordinates all layers are treated equally while using z coordinate the surface layer is special. Finally, the z^* coordinate is clearly a more natural coordinate than height for examining the interaction between barotropic and baroclinic modes. Indeed, we suspect that z^* is likely to be a more natural coordinate than z for most applications whether the free-surface amplitudes are large or not.

4. Discussion

We have presented the z^* coordinate, first used by Stacey et al. (1995), as an alternative vertical coordinate for height-coordinate models with a free surface. Combining the use of this coordinate with the finite volume representation of topography (Adcroft et al., 1997) yields an accurate representation of barotropic dynamics over topography. Although the emphasis here has been on numerical modeling, the illustration given suggests that the z^* coordinate is a useful framework for thinking more generally about 3D motions with a divergent barotropic component.

The motivation for adopting the z^* coordinate was primarily driven by the moving boundary problem represented by the free surface. Although we are quite satisfied with the non-linear free-surface implementation of Campin et al. (in press) it does not address the issue of a vanishing surface layer. As mentioned, this problem becomes more pressing as the vertical resolution is increased. Adopting the z^* coordinate has transformed the moving physical domain into a fixed computational domain. Using z^* also leads to a cleaner separation of the external and internal modes of variability; the vertical advection associated with the external mode is treated in a Lagrangian manner.

We must emphasize the close connection between z^* and height; recall that z^* only differs from z when the free-surface elevation is non-zero. For a deep ocean, the slope of z^* coordinate surfaces is very small (of order $(\nabla\eta)/H$ near the surface, linearly tapering to zero at the bottom). The apparent connection to terrain following coordinates is only incidental; z^* only looks similar to σ -coordinates for the special case of a flat bottom.

Stacey et al. (1995) called the coordinate “coastal” but we speculate that use of the z^* coordinate would allow the inclusion of tides in global scale circulation models without deleterious effects; adding tides to conventional height coordinate global models would lead to spurious

diapycnal diffusion due to the relatively large, high-frequency vertical flow associated with tides. The case for explicitly forcing tides in *coarse* resolution global models is unclear. However, there is a strong chance that at high resolutions, $O(10\text{ km})$, exchange processes with marginal and coastal seas could begin to be resolved and might strongly be affected by the presence of explicit tides.

As mentioned, the oceanographic z^* coordinate is isomorphic with the meteorological η coordinate. The MIT model takes advantage of an isomorphism between Boussinesq equations in height coordinates and the non-Boussinesq equations in pressure coordinates (Marshall et al., submitted). This $z - p$ isomorphism has allowed the same hydrodynamical kernel to be employed to model the non-Boussinesq ocean and atmosphere (equations in p coordinates) in addition to modeling the Boussinesq ocean (in z coordinates). For instance, Losch et al. (in press) used the $z - p$ isomorphism to demonstrate that non-Boussinesq effects are inconsequential in coarse resolution models. One argument why this had to be true was the similarity between the z and p coordinate equations (structurally the same) with one exception which was the location of the moving boundary. The same extensions apply to the $z^* - p^*$ isomorphism (given in Appendix B for reference) allowing the model to solve the hydrostatic non-Boussinesq compressible equations for the ocean. Here, however, because the moving domain has been mapped into a fixed computational domain, the structural similarities between the z^* and p^* coordinate equations is absolute. We therefore speculate that Losch et al. (in press) would find even smaller discrepancies between the Boussinesq and non-Boussinesq models.

The MIT model in height coordinates (Marshall et al., 1997b) also has a non-hydrostatic capability that allows one to relax the hydrostatic balance assumption in the vertical momentum equation. The non-hydrostatic equations of motion are most naturally written in height coordinates and writing them in any other coordinate introduces terms that are complicated enough to require approximation of the equations rendering “quasi-non-hydrostatic” models (Miller and White, 1984; White, 1989). Here, if we were to write the non-hydrostatic equations in z^* coordinates we expect the new terms to be proportional to the coordinate slope and thus relatively small. By introducing these terms in our height based non-hydrostatic algorithm we hope to produce a non-hydrostatic model in z^* coordinates that would be well suited for coastal scale applications. This is work for the future.

Acknowledgements

The authors would like to thank the anonymous reviewers and the editor for their constructive comments.

Appendix A. Transforming the equations of motion into general coordinates

This derivation follows that of Kasahara (1974) and Bleck (1978a,b, 2002) but here we place the emphasis on interpretation from the height coordinate perspective rather than a hybrid perspective. The hydrostatic and incompressible Boussinesq equations of motion in height coordinates for the ocean are

$$D_t \vec{v}_h + f \hat{k} \wedge \vec{v}_h + \frac{1}{\rho_0} \nabla_z p = \vec{F} \quad (\text{A.1})$$

$$g \rho + \partial_z p = 0 \quad (\text{A.2})$$

$$\nabla_z \cdot \vec{v}_h + \partial_z w = 0 \quad (\text{A.3})$$

$$D_t \theta = Q_\theta \quad (\text{A.4})$$

$$D_t s = Q_s \quad (\text{A.5})$$

$$\rho = \rho(\theta, s, p) \quad (\text{A.6})$$

where $D_t \equiv [\partial_t + \vec{v}_h \cdot \nabla_h + w \partial_z]$ is the total derivative, $\vec{v}_h = (u, v, 0)$ is the horizontal component of flow, $w = D_t z$ is the vertical flow, p is the fluid pressure, θ is the potential temperature, s is the salinity, ρ is the (in situ) density, \vec{F} are accelerations due to divergences of stresses, Q_θ and Q_s represent sources and sinks of heat and salinity. g is the constant acceleration due to gravity, ρ_0 is a constant representing an average density, f is the Coriolis parameter and can be a function of horizontal coordinates. In the above equations the horizontal gradient operator, ∇_h , is used and denoted with the subscript “ h ” to distinguish it from gradients taken along other coordinate surfaces to be introduced later. The boundary conditions are as follows. At the solid bottom, $z = -H(x, y)$, there is no normal flow so that

$$w = -\vec{v}_h \cdot \nabla H \quad \text{at } z = -H(x, y)$$

and at the free surface, $z = \eta(x, y, t)$, we impose the kinematic condition

$$w = D_t \eta - (P - E)$$

where $P - E$ is the net precipitation minus evaporation. The incompressible continuity equation can be integrated over the fluid thickness, $H + \eta$, and using the top and bottom boundary conditions on w yield the free-surface equation

$$\partial_t \eta + \nabla \cdot [(\eta + H) \langle \vec{v}_h \rangle] = P - E$$

where $\langle \vec{v}_h \rangle$ is the depth averaged horizontal flow.

A.1. Rules of transformation

To transform the above equations into an arbitrary coordinate “ r ” we make use of the following relations. For an arbitrary scalar field, A , which is invariant to a coordinate transformation, we have

$$A(x, y, z, t) = A(x, y, z(x, y, r, t), t)$$

where $r = r(x, y, z, t)$ is the new vertical coordinate which can be expressed as a smooth function of space, time and model state variables. Thus, in vector notation, horizontal gradient and divergence operators become

$$\nabla_z A = \nabla_r A - \left. \frac{\partial r}{\partial z} \right|_{xyt} \left. \frac{\partial A}{\partial r} \right|_{xyt} \nabla_r z$$

$$\nabla_z \cdot \vec{v}_h = \nabla_r \cdot \vec{v}_h - \frac{\partial r}{\partial z} \Big|_{xyt} \frac{\partial \vec{v}_h}{\partial r} \Big|_{xyt} \cdot \nabla_r z$$

and the total derivative in (x, y, r, t) coordinates is

$$D_t A = \frac{\partial A}{\partial x} \Big|_{yrt} D_t x + \frac{\partial A}{\partial y} \Big|_{xrt} D_t y + \frac{\partial A}{\partial r} \Big|_{xyt} D_t r + \frac{\partial A}{\partial t} \Big|_{xyr} D_t t = u \frac{\partial A}{\partial x} \Big|_{yrt} + v \frac{\partial A}{\partial y} \Big|_{xrt} + \dot{r} \frac{\partial A}{\partial r} \Big|_{xyt} + \frac{\partial A}{\partial t} \Big|_{xyr}$$

where $\dot{r} = D_t r$ is the vertical velocity in r coordinates.

A.2. Term by term transformation

Using the above relations we can transform terms in the z coordinate equations of motion as follows. The hydrostatic balance equation becomes

$$g\rho + \frac{\partial p}{\partial z} \Big|_{xyt} = g\rho + \frac{\partial p}{\partial r} \Big|_{xyt} \frac{\partial r}{\partial z} \Big|_{xyt} = 0$$

which is better written

$$\rho \frac{\partial}{\partial r} \Big|_{xyt} (gz) + \frac{\partial p}{\partial r} \Big|_{xyt} = 0$$

The horizontal pressure gradient term becomes

$$\nabla_z p = \nabla_r p - \frac{\partial r}{\partial z} \Big|_{xyt} \frac{\partial p}{\partial r} \Big|_{xyt} \nabla_r z = \nabla_r p + \rho \nabla_r (gz)$$

In the incompressible continuity equation we must transform $\partial_z w$ and to do this we use the definition of w in r coordinates:

$$w = D_t z = \frac{\partial z}{\partial t} \Big|_{xyr} + u \frac{\partial z}{\partial x} \Big|_{yrt} + v \frac{\partial z}{\partial y} \Big|_{xrt} + \dot{r} \frac{\partial w}{\partial z} \Big|_{xyt}$$

so that

$$\begin{aligned} \frac{\partial w}{\partial z} \Big|_{xyt} &= z_r^{-1} \frac{\partial w}{\partial r} \Big|_{xyt} \\ &= z_r^{-1} \left[\frac{\partial}{\partial t} \Big|_{xyr} z_r + u \frac{\partial}{\partial x} \Big|_{yrt} z_r + v \frac{\partial}{\partial y} \Big|_{xrt} z_r + \dot{r} \frac{\partial}{\partial r} \Big|_{xyt} z_r + \frac{\partial}{\partial r} \Big|_{xyt} \vec{v}_h \cdot \nabla_r z + z_r^{-1} \frac{\partial}{\partial r} \Big|_{xyt} \dot{r} \right] \\ &= z_r^{-1} \left[D_t z_r + \frac{\partial \vec{v}_h}{\partial r} \Big|_{xyt} \cdot \nabla_r z + z_r \frac{\partial \dot{r}}{\partial r} \Big|_{xyt} \right] \end{aligned}$$

where we use the notation z_r for the thickness

$$z_r \equiv \frac{\partial z}{\partial r} \Big|_{xyt}$$

The non-divergence of flow leads to a continuity equation for thickness in r coordinates

$$z_r[\nabla_z \cdot \vec{v}_h + \partial_z w] = D_t z_r + z_r(\nabla_r \cdot \vec{v}_h + \partial_r \dot{r}) = 0$$

or

$$\partial_t z_r + \nabla_r \cdot z_r \vec{v}_h + \partial_r z_r \dot{r} = 0$$

The use of Lagrangian derivatives (D_t) has been convenient during the transformation of coordinates but it is more useful to use a flux form of advection to more easily ensure global conservation. For an arbitrary scalar, θ , the total derivative can be transformed as follows:

$$z_r D_t \theta = D_t(z_r \theta) - \theta D_t z_r = D_t(z_r \theta) + \theta z_r[\nabla_r \cdot \vec{v}_h + \partial_r \dot{r}] = \partial_t(z_r \theta) + \nabla_r \cdot (z_r \theta \vec{v}_h) + \partial_r(z_r \theta \dot{r})$$

Using the above relations, the hydrostatic Boussinesq equations of motion transformed to r coordinates are

$$D_t \vec{v}_h + f \hat{k} \wedge \vec{v}_h + \frac{1}{\rho_0} \nabla_r p + \frac{\rho}{\rho_0} \nabla_r(gz) = \vec{F} \tag{A.7}$$

$$\rho \partial_r(gz) + \partial_r p = 0 \tag{A.8}$$

$$\partial_t z_r + \nabla_r \cdot (z_r \vec{v}_h) + \partial_r(z_r \dot{r}) = 0 \tag{A.9}$$

$$\partial_t(z_r \theta) + \nabla_r \cdot (z_r \theta \vec{v}_h) + \partial_r(z_r \theta \dot{r}) = Q_\theta \tag{A.10}$$

$$\partial_t(z_r s) + \nabla_r \cdot (z_r s \vec{v}_h) + \partial_r(z_r s \dot{r}) = Q_s \tag{A.11}$$

$$\rho = \rho(\theta, s, p) \tag{A.12}$$

In the above equations, this is the scale factor, z_r , that discriminates between different coordinate systems (choices of r). If we choose $r = z$ then $z_r = 1$ and we recover the original height coordinates equations. If we choose $r = \sigma = (z - \eta)/(H + \eta)$ then $z_r = H + \eta$. The subject of this paper is the rescaled height coordinate, $r = z^* = \sigma H$, for which $z_r = (H + \eta)/H$ leading to Eqs. (9)–(13).

A.3. Free-surface equation in a general coordinate model

Note that integrating the continuity equation over the fluid depth predicts the fluid thickness

$$\int_{r(z=-H)}^{r(z=\eta)} z_r dr = \eta + H$$

and so should recover the surface elevation equation which should be independent of the vertical coordinate system. To verify this we need the boundary conditions on \dot{r} which may be simple for given choices of coordinate but are non-trivial for general coordinates. First we note that for a functional form of the vertical coordinate, $z = z(r, \eta, H)$ we can relate w to \dot{r} using the chain rule:

$$w \equiv D_t z(r, \eta, H) = z_r \dot{r} + z_\eta D_t \eta + z_H D_t H$$

where $z_r = \partial_r|_{\eta, H} z$, $z_\eta = \partial_\eta|_{r, H} z$ and $z_H = \partial_H|_{r, \eta} z$. Applying $w = D_t \eta - (P - E)$ at the surface, $z = \eta$, gives

$$z_r \dot{r} = (1 - z_\eta) D_t \eta - z_H D_t H - (P - E) \quad \text{at } r = r_t = r(z = \eta)$$

and applying $w = -D_t H$ at the bottom, $z = -H$, gives

$$z_r \dot{r} = -z_\eta D_t \eta - (1 + z_H) D_t H \quad \text{at } r = r_b = r(z = -H).$$

Note there is no choice of $z = z(r, \eta, H)$ that can avoid the appearance of $P - E$ in the surface boundary condition. An optimal choice of $z(r)$ would have $z_\eta(z = \eta) = 0$ and $z_H(z = \eta) = 0$ at the surface and $z_\eta(z = -H) = 0$ and $1 + z_H(z = -H) = z_r(z = -H)$ at the bottom, thereby simplifying the form of these boundary conditions.

Substituting the above boundary conditions at the top and the bottom for $z_r \dot{r}$ and using Leibniz rule gives the familiar free-surface height equation

$$\partial_t \eta + \nabla \cdot [(\eta + H) \langle \vec{v}_h \rangle] = P - E \quad (\text{A.13})$$

Appendix B. Atmospheric η and oceanic p^* coordinates

Through the isomorphism between oceanic and atmospheric equations of motion (Marshall et al., submitted), the algorithm used to solve the oceanic equations (given in Appendix A) can also be used to solve the non-Boussinesq, hydrostatic, atmospheric equations of motion in pressure coordinates which are:

$$D_t \vec{v}_h + f \hat{k} \wedge \vec{v}_h + \nabla_p \Phi = \vec{F} \quad (\text{B.1})$$

$$\alpha + \partial_p \Phi = 0 \quad (\text{B.2})$$

$$\nabla_p \cdot \vec{v}_h + \partial_p \omega = 0 \quad (\text{B.3})$$

$$D_t \theta = Q_\theta \quad (\text{B.4})$$

$$D_t q = Q_q \quad (\text{B.5})$$

$$\alpha = \theta \partial_p \Pi \quad (\text{B.6})$$

where $\Pi(p)$ is the Exner function, $\omega = D_t p$ is the vertical velocity in pressure coordinates, α is specific volume, $\Phi = gz$ is the geopotential and q is specific humidity. The boundary conditions are

$$\omega = 0 \quad \text{at } p = 0 \text{ (the top)} \quad (\text{B.7})$$

and

$$\omega = D_t p_s \quad \text{at } p = p_s(x, y, t) \text{ (the ground)} \quad (\text{B.8})$$

Integrating the continuity equation between top and bottom in pressure gives the surface pressure equation:

$$\partial_t p_s + \nabla \cdot [p_s \langle \vec{v}_h \rangle] = 0 \quad (\text{B.9})$$

Transforming to an arbitrary vertical coordinate, r , following the derivation given earlier for the height-coordinate Boussinesq equations, gives:

$$D_t \vec{v}_h + f \hat{k} \wedge \vec{v}_h + \alpha \nabla_r p + \nabla_r \Phi = \vec{F} \quad (\text{B.10})$$

$$\partial_r \Phi + \alpha \partial_r p = 0 \quad (\text{B.11})$$

$$\partial_t p_r + \nabla_r \cdot (p_r \vec{v}_h) + \partial_r (p_r \dot{r}) = 0 \quad (\text{B.12})$$

$$\partial_t (p_r \theta) + \nabla_r \cdot (p_r \theta \vec{v}_h) + \partial_r (p_r \theta \dot{r}) = Q_\theta \quad (\text{B.13})$$

$$\partial_t(p_r q) + \nabla_r \cdot (p_r q \vec{v}_h) + \partial_r(p_r q \dot{r}) = Q_q \quad (\text{B.14})$$

$$\alpha = \theta \partial_p \Pi \quad (\text{B.15})$$

Now we choose the vertical coordinate to be the atmospheric η coordinate which we define

$$r = p^* = \sigma p_s^o = \frac{p}{p_s^o} \quad (\text{B.16})$$

Here on, we will use the symbol p^* rather than the conventional symbol η for the vertical coordinate to avoid confusion with the dependent variable used in the oceanic equations. This will also remind us that the p^* takes the same form as the rescaled height coordinate z^* and at the same time is most closely related to pressure, p . The common factor required to describe the coordinate transformation is

$$\partial_{p^*} p = \frac{p_s}{p_s^o}$$

so that the equations of motion using p^* as the vertical coordinate becomes

$$D_t \vec{v}_h + f \hat{k} \wedge \vec{v}_h + \alpha \nabla_{p^*} p + \nabla_{p^*} \Phi = \vec{F} \quad (\text{B.17})$$

$$\partial_{p^*} \Phi + \alpha \frac{p_s}{p_s^o} = 0 \quad (\text{B.18})$$

$$\partial_t \frac{p_s}{p_s^o} + \nabla_{p^*} \cdot \left(\frac{p_s}{p_s^o} \vec{v}_h \right) + \partial_{p^*} \left(\frac{p_s}{p_s^o} \dot{r} \right) = 0 \quad (\text{B.19})$$

$$\partial_t \left(\frac{p_s}{p_s^o} \theta \right) + \nabla_{p^*} \cdot \left(\frac{p_s}{p_s^o} \theta \vec{v}_h \right) + \partial_{p^*} \left(\frac{p_s}{p_s^o} \theta \dot{r} \right) = Q_\theta \quad (\text{B.20})$$

$$\partial_t \left(\frac{p_s}{p_s^o} q \right) + \nabla_{p^*} \cdot \left(\frac{p_s}{p_s^o} q \vec{v}_h \right) + \partial_{p^*} \left(\frac{p_s}{p_s^o} q \dot{r} \right) = Q_q \quad (\text{B.21})$$

$$\alpha = \theta \partial_{p^*} \Pi \quad (\text{B.22})$$

To apply these equations to the non-Boussinesq ocean (following Losch et al., in press), we simply replace q by s and the ideal gas equation (B.22) with

$$\alpha = \alpha(s, \theta, p) \quad (\text{B.23})$$

References

- Adcroft, A., Hill, C., Marshall, J., 1997. Representation of topography by shaved cells in a height coordinate ocean model. *Mon. Wea. Rev.* 125, 2293–2315.
- Bleck, R., 1978a. Finite difference equations in generalized vertical coordinates. Part I: Total energy conservation. *Contrib. Atmos. Phys.* 51, 360–372.
- Bleck, R., 1978b. On the use of hybrid vertical coordinates in numerical weather prediction models. *Mon. Wea. Rev.* 106 (9), 1233–1244.
- Bleck, R., 2002. An oceanic general circulation model framed in hybrid isopycnic-Cartesian coordinates. *Ocean Modell.* 37, 55–88.

- Bleck, R., Rooth, C., Hu, D., Smith, L., 1992. Ventilation patterns and mode water formation in a wind- and thermodynamically driven isopycnic coordinate model of the North Atlantic. *J. Phys. Oceanogr.* 22, 1486–1505.
- Campin, J.-M., Adcroft, A., Hill, C., Marshall, J., in press. Conservation of properties in a free-surface model. *Ocean Modell.* 6, 221–244.
- Dukowicz, J., Dvinsky, A., 1993. A reformulation and implementation of the Bryan–Cox–Semtner ocean model on the connection machine. *J. Ocean. Atmos. Tech.* 10, 195–208.
- Griffies, S., Harrison, M., Pacanowski, R., Rosati, A., 2003. A technical guide to MOM4. NOAA/Geophysical Fluid Dynamics Laboratory.
- Griffies, S., Pacanowski, R., Schmidt, M., Balaji, V., 2001. Tracer conservation with an explicit free-surface method for z-coordinate ocean models. *Mon. Wea. Rev.* 129, 1081–1098.
- Haidvogel, D., Arango, H., Kedstrom, K., Beckmann, A., Malanotte-Rizzoli, P., Shchepetkin, A., 2000. Model evaluation experiments in the North Atlantic Basin: simulations in nonlinear terrain-following coordinates 32 (3–4), 239–281.
- Hallberg, R., 1997. Stable split time stepping schemes for large-scale ocean modelling. *JCP* 135, 54–65.
- Haney, R., 1991. On the pressure-gradient force over step topography in sigma coordinate ocean models. *J. Phys. Oceanogr.* 21 (4), 610–619.
- Hundsdorfer, W., Koren, B., van Loon, M., Verwer, J., 1995. A positive finite-difference advection scheme. *J. Comput. Phys.* 117, 35–46.
- Janjic, Z., 1977. Pressure gradient force and advection scheme used for forecasting with steep and small scale topography. *Contrib. Atm. Phys.* 50, 186–199.
- Kasahara, A., 1974. Various vertical coordinate systems used for numerical weather prediction. *Mon. Wea. Rev.* 102 (7), 509–522.
- Killworth, P.D., Stainforth, D., Webb, D.J., Peterson, S.M., 1991. The development of a free-surface Bryan–Cox–Semtner model. *J. Phys. Oceanogr.* 21, 1333–1348.
- Losch, M., Adcroft, A., Campin, J.-M., in press. How sensitive are coarse general circulation models to fundamental approximations in the equations of motion? *J. Phys. Oceanogr.*
- Marshall, J., Adcroft, A., Hill, C., Campin, J.-M., submitted. Fluid isomorphisms in climate modeling. *J. Clim.*
- Marshall, J., Adcroft, A., Hill, C., Perelman, L., Heisey, C., 1997a. A finite-volume, incompressible Navier–Stokes model for studies of the ocean on parallel computers. *J. Geophys. Res.* 102 (C3), 5753–5766.
- Marshall, J., Hill, C., Perelman, L., Adcroft, A., 1997b. Hydrostatic, quasi-hydrostatic, and nonhydrostatic ocean modeling. *J. Geophys. Res.* 102 (C3), 5733–5752.
- Mesinger, F., Jancic, Z.I., Mickovic, S., Gavrillov, D., 1988. The step-mountain coordinate: model description and performance for cases of alpine lee cyclogenesis and for a case of an Appalachian redevelopment. *Mon. Wea. Rev.* 116, 1493–1518.
- Miller, M., White, A., 1984. On the non-hydrostatic equations in pressure and sigma coordinates. *Quart. J. R. Meteorol. Soc.* 110 (464), 515–533.
- Pacanowski, R., Gnanadesikan, A., 1998. Transient response in a z-level ocean model that resolves topography with partial-cells. *Mon. Wea. Rev.* 126, 3248–3270.
- Pietrzak, J., 1998. The use of TVD limiters for forward-in-time upstream-biased advection schemes in ocean modeling. *Mon. Wea. Rev.* 126, 812–830.
- Smith, R., Dukowicz, J., Malone, R., 1992. Parallel ocean general circulation modelling. *Physica D* 60, 38–61.
- Song, Y., submitted for publication. Computational design of the generalized coordinate ocean model for multi-scale compressible or incompressible flow applications, JAOT.
- Song, Y., Haidvogel, D., 1994. A semi-implicit ocean circulation model using a generalized topography-following coordinate system. *J. Comput. Phys.* 115, 546–560.
- Stacey, M.W., Gratton, Y., 2001. The energetics and tidally induced reverse renewal in a two-silled Fjord. *J. Phys. Oceanogr.* 31, 1599–1615.
- Stacey, M.W., Pond, S., Nowak, Z.P., 1995. A numerical model of the circulation in knight inlet, British Columbia, Canada. *J. Phys. Oceanogr.* 25, 1037–1062.
- White, A., 1989. An extended version of a non-hydrostatic, pressure coordinate model. *Quart. J. R. Meteorol. Soc.* 115 (490), 1243–1251.